Wan *et al*. *Dis Prev Res* 2023;2:8
DOI: 10.20517/dpr.2023.13

Disaster Prevention and Resilience

Research Article

Open Access

Check for updates

Fréchet-derivative-based global sensitivity analysis of the physical random function model of ground motions

Zhiqiang Wan[1], Weifeng Tao[1], Yanqiong Ding[2], Lifeng Xin[1]

[1]School of Mechanics, Civil Engineering and Architecture, Northwestern Polytechnical University, Xi'an 710072, Shaanxi, China.
[2]School of Civil Engineering, Xi'an University of Architecture and Technology, Xi'an 710055, Shaanxi, China.

Correspondence to: Assoc. Prof. Dr. Zhiqiang Wan, School of Mechanics, Civil Engineering and Architecture, Northwestern Polytechnical University, Xi'an 710072, Shaanxi, China. E-mail: wanzhiqiang@nwpu.edu.cn; ORCID: 0000-0003-2973-0042

How to cite this article: Wan Z, Tao W, Ding Y, Xin L. Fréchet-derivative-based global sensitivity analysis of the physical random function model of ground motions. *Dis Prev Res* 2023;2:8. http://dx.doi.org/10.20517/dpr.2023.03

Received: 22 Apr 2023 **First Decision:** 22 May 2023 **Revised:** 25 May 2023 **Accepted:** 1 Jun 2023 **Published:** 14 Jun 2023

Academic Editor: Jun Xu **Copy Editor:** Fanglin Lan **Production Editor:** Fanglin Lan

Abstract

Randomness in earthquake ground motions is prevalent in real engineering practices. Therefore, it is of paramount significance to utilize an appropriate model to simulate random ground motions. In this paper, a physical random function model of ground motions, which considers the source-path-site mechanisms of earthquakes, is employed for the seismic analysis. The probability density evolution method is adopted to quantify the extreme value distribution of structural responses. Then, the sensitivity analysis of the extreme value distribution with respect to basic model parameters is conducted via a newly developed Fréchet-derivative-based approach. A 10-story reinforced concrete frame structure, with nominal deterministic structural parameters and subjected to random ground motions, is studied. The results indicate that when the structure is still in a linear or weakly nonlinear stage in the situation of frequent earthquakes, the model parameter called the equivalent predominate circular frequency is of the most significance, with an importance measure (IM) greater than 0.8. Nonetheless, if the structure exhibits strong nonlinearity, such as in the case of a rare earthquake, the equivalent predominate circular frequency remains highly influential, but the Brune source parameter, which describes the decay process of the fault rupture, becomes important as well, with an IM increased from around 0.2 to around 0.4. These findings indicate that the IMs of basic model parameters are closely related to the embedded physical mechanisms of the structure, and the change in the physical state of the structure may provoke the change of IMs of basic inputs. Furthermore, some other issues are also outlined.

Keywords: Uncertainty quantification, sensitivity analysis, seismic analysis, probability density evolution method

1. INTRODUCTION

In practical applications, quantification of various engineering uncertainties has become one of the most crucial concerns in the process of structural design and analysis. In general, considering the difference in sources of uncertainty, uncertainty can be categorized into two aspects[1–5]: (1) the natural variability from the structural parameters, such as the uncertainty in mechanical properties of structural materials, geometric parameters, model discrepancies, etc., and (2) the randomness of external excitations, such as earthquake ground motions. Although considering both the randomness of ground motions and the structural parameters is the most objective[6,7], it may be more convenient for the preliminary structural design and evaluation to only take into account the randomness of ground motions[8–10]. In this view, only the uncertainty of ground motions is focused on in this work.

For seismic analysis, the simulation of ground motions plays a significant role in the dynamical analysis of structures, especially when typical earthquake records of past strong ground motions may not be available for most engineering sites. To this end, numerous ground-motion models have been developed in the past decades, mainly by following three distinct pathways. The first path belongs to the category of seismology models[11–14], which predicts the earthquake ground motions by modeling the physical mechanisms, including the source, propagation medium, etc. The second and perhaps the most classical path in the engineering field is to adopt a given response spectrum or a power spectrum, on which a lot of fundamental and representative works have been done by Housner (1947)[15], Kanai (1957)[16] and Tajimi (1960)[17], Hu and Zhou (1962)[18], Ou and Niu (1990)[19], Clough and Penzien (1995)[20], etc. This approach falls within the scope of engineering models, which aim at describing the second-order statistic characteristics of earthquakes from ground-motion records, and the non-stationarity of earthquakes is simulated by adopting a modulated function in the time domain[21,22]. Different from seismology models, engineering models are more concerned with the influence of engineering sites on the ground motion. However, it has been confirmed that the physical mechanisms of the source and the complex propagation path also have critical impacts on the seismic response of engineering structures. For this reason, the third path is to combine the benefits of seismology models and engineering models, known as engineering seismic models, which focus on onshore earthquakes[23–26] and offshore earthquakes[27–30]. Considering the local site effect, Li and Ai (2006)[31] proposed the idea of a physical random function model to reconstruct non-stationary stochastic ground motions. Building on this foundation, Wang and Li (2011)[23] developed a physical random function model of ground motions (hereinafter referred to as "StoModel"). This model incorporates the randomness of the source and the site through four random variables that have specific physical interpretations. Then, the distributions of these four random variables can be identified based on actual earthquake records[32]. Nevertheless, it is found that the distribution parameters of the random variables in StoModel may be significantly different[33] when the statistical uncertainty from data of ground motions is involved. Therefore, there is a need to establish a more robust StoModel that holds the capability to reflect the randomness of earthquakes under various conditions of data. It should be emphasized that the adopted StoModel may not be the best ground-motion model currently available, but it is simple enough to help illustrate the present work in this paper.

In fact, the robustness of a stochastic model can be partially enhanced through the application of the global sensitivity analysis (GSA)[34]. For instance, setting non-influential input variables of a stochastic model to nominal values would help decrease the statistical uncertainty arising from data, thereby enhancing the practical robustness. One of the quantitative measures in the GSA is the global sensitivity index (GSI). Among a variety of GSIs, the variance-based Sobol' index[35,36] and the moment-independent index[37,38] are two popular GSIs that have been applied in structural engineering[39], aerospace engineering[40], geotechnical engineering[41], and other fields. The variance-based GSI measures the contribution of each basic input (or the interaction effect of two or more inputs) on the variance of the quantity of interest (QoI), while the moment-independent GSI is defined on the stochastic distance between unconditional distribution and conditional distribution. Apparently, these two indices are always non-negative, indicating that they do not provide information about the direction of sensitivity. As a result, there is a risk of being misled into assuming that an increase in the uncertainty of inputs will invariably result in an increase in the uncertainty of outputs. In fact, the direction of sensitivity might be more essential than the importance measure (IM) when dealing with particular issues of engineering. For instance, the failure-probability-based GSI, defined as the derivative of failure probability with respect to basic distribution parameters, plays a crucial role in reliability-based design optimization[42]. While GSA is supposed to provide adequate information for revealing the global physical features of stochastic systems, it is noticed that considering only second-order moments or failure probability may not be adequate. Therefore, it is reasonable to adopt a GSI that can effectively capture both the IM and the direction of sensitivity with respect to the probability distribution, rather than solely relying on second-order moments or failure probability.

In this paper, We conduct the GSA of StoModel using a Fréchet-derivative-based approach[43]. The Fréchet-derivative-based GSI (Fre-GSI) is employed as the measure. To reduce computational costs associated with calculating the Fre-GSIs, we incorporate the probability density evolution method (PDEM) and the change of probability measure (COM)[4]. To investigate the GSA of structural responses to basic random variables in StoModel, we use a typical high-rise reinforced concrete structure as the benchmark. The results of Fréchet-derivative-based GSA (Fre-GSA) provide insights into improving the robustness of the StoModel, and these improvements are discussed in detail.

2. METHODS

2.1 Physical random function model of ground motions

The StoModel studied in this research is based on the source-path-site mechanisms. Specifically, this model consists of two physical models: the amplitude spectrum model $A_R(\boldsymbol{\Theta}, \omega)$ and the phase spectrum model $\Phi_R(\boldsymbol{\Theta}, \omega)$. Then, at a point on the surface of a specific local engineering site with the epicentral distance of R, the acceleration of ground motion can be generated by[23]

$$a_R(\boldsymbol{\Theta}, t) = \frac{1}{2\pi} \int_{-\infty}^{+\infty} A_R(\boldsymbol{\Theta}, \omega) \cos\left(\omega t + \Phi_R(\boldsymbol{\Theta}, \omega)\right) \mathrm{d}\omega \tag{1}$$

where the amplitude spectrum model $A_R(\boldsymbol{\Theta}, \omega)$ is given by

$$A_R(\boldsymbol{\Theta}, \omega) = A_0 \frac{\omega e^{-K\omega R}}{\sqrt{\omega^2 + (1/\tau)^2}} \times \sqrt{\frac{1 + 4\zeta_g^2 \left(\omega/\omega_g\right)^2}{\left[1 - \left(\omega/\omega_g\right)^2\right]^2 + 4\zeta_g^2 \left(\omega/\omega_g\right)^2}} \tag{2}$$

where $K = 10^{-5}$ s/km is the attenuation parameter, and the phase spectrum model reads

$$\Phi_R(\boldsymbol{\Theta}, \omega) = \arctan\left(\frac{1}{\tau\omega}\right) - \ln\left[(a + 0.5)\omega + b + \frac{1}{4c}\sin(2c\omega)\right] Rd. \tag{3}$$

In the StoModel, A_0 is the amplitude parameter of the source, τ is the Brune source parameter describing the decay process of the fault rupture, ζ_g is the equivalent damping ratio of the site, and ω_g is the equivalent predominate circular frequency of the site. On the consideration of physical interpretations of the parameters $\{A_0, \tau, \zeta_g, \omega_g\}$, it is appropriate to denote $\boldsymbol{\Theta} = [A_0, \tau, \zeta_g, \omega_g]$ as the basic random source that characterizes the uncertainty of ground motions. It should be emphasized that the remaining parameters $\{a, b, c, d, R\}$, which have a crucial impact on the phase spectrum model, may also possess randomness. However, to clearly illustrate the proposed method in this paper, these parameters are assumed to be deterministic by setting $a = 1.02$, $b = 403$, $c = 1.89$, $d = 130$, and $R = 20$ km, as referenced from Wang & Li (2012)[24]. The reader interested in the randomness of $\{a, b, c, d, R\}$ is directed to Ding *et al.* (2018, 2022)[25,26] for further information.

Table 1. Probabilistic information of the physical random function model of ground motions [32]

Random variable	Distribution type	Site	Distribution parameters	
		Site	a_1	b_1
A_0	Lognormal	I	−1.4306	0.9763
		II	−1.2712	0.8267
		III	−1.1047	0.7388
		IV	−0.9280	0.6380
		Site	a_2	b_2
τ	Lognormal	I	−1.3447	1.4724
		II	−1.2403	1.3436
		III	−1.1574	1.1341
		IV	−0.9712	1.0553
		Site	a_3	b_3
ζ_g	Gamma	I	3.9368	0.1061
		II	5.1326	0.0800
		III	6.1838	0.0689
		IV	6.4089	0.0658
		Site	a_4	b_4
ω_g	Gamma	I	2.0994	9.9279
		II	2.2415	7.4136
		III	2.0866	5.6598
		IV	1.9401	5.5265

According to the site classification recommended in the Chinese code for seismic design of buildings (GB 50011-2010)[44], the marginal probability density functions (PDFs) of $\{A_0, \tau, \zeta_g, \omega_g\}$ are estimated[32] using a database of 4438 seismic ground motions from the Pacific Earthquake Engineering Research Center (PEER). The assumption of Independence is made by $\{A_0, \tau, \zeta_g, \omega_g\}$, and the probabilistic information of $\{A_0, \tau, \zeta_g, \omega_g\}$ is summarized in Table 1. The PDFs of $\{A_0, \tau, \zeta_g, \omega_g\}$ for Site I, Site II, Site III, and Site IV are shown in Figure 1.

It is evident that the distribution parameters of basic random sources vary greatly for different site classes. This variation can be attributed to both the physical characteristics of different site classes and the statistical uncertainty originating from the earthquake ground motions. In other words, the distribution parameters derived from the analysis of 4438 seismic ground motions[32] may possess epistemic uncertainty, as demonstrated in the study by Li & Liu (2015)[33] where different distribution parameters are estimated from the records of 2008 Wenchuan earthquakes. To this regard, it is valuable to study how these uncertainties may affect the uncertainty of structural responses, such as maximum inter-story drift angle, top displacement, etc.

In Table 1, the PDFs of Lognormal distribution and Gamma distribution are given by

$$\begin{cases} \text{Lognormal: } p_{\Theta_i}(\theta_i; a_i, b_i) = \dfrac{1}{\sqrt{2\pi} b_i \theta_i} \exp\left(-\dfrac{(\ln \theta_i a_i)^2}{2b_i^2}\right), \ i = 1, 2, \\ \text{Gamma: } p_{\Theta_j}(\theta_j; a_j, b_j) = \dfrac{1}{\Gamma(a_j) b_j^{a_j}} \theta_j^{a_j - 1} \exp\left(-\dfrac{\theta_j}{b_j}\right), \ j = 3, 4. \end{cases} \tag{4}$$

Besides, for the sake of simplicity, the distribution parameters in Table 1 are numbered in order as follows: $\{a_1, b_1\}$ for $A_0 = \Theta_1$, $\{a_2, b_2\}$ for $\tau = \Theta_2$, $\{a_3, b_3\}$ for $\zeta_g = \Theta_3$, and $\{a_4, b_4\}$ for $\omega_g = \Theta_4$, for Site I to Site IV.

2.2. Uncertainty propagation via the probability density evolution method

In this section, We introduce the basic theory and numerical algorithm of the PDEM[45], which is adopted to estimate the PDF of the QoI.

Without loss of generality, Let us consider a MDOF structure with the equation of motion given by:

$$\mathbf{M} \ddot{X} + \mathbf{C} \dot{X} + \mathbf{f}(X) = \xi a_R(\mathbf{\Theta}, t) \tag{5}$$

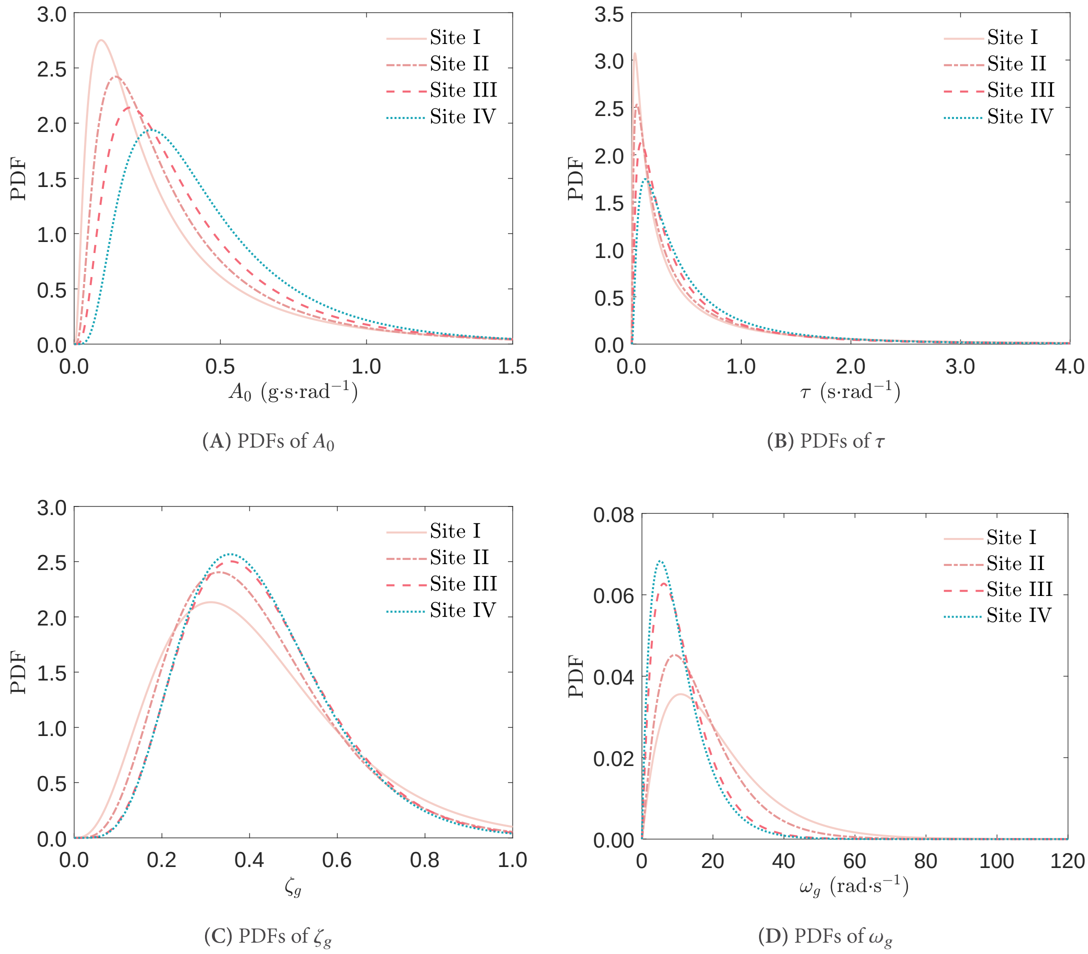

Figure 1. PDFs of parameters of physical random function model of ground motions according to the site classification in the Chinese design code (GB 50011-2010)[44].

where $\mathbf{M}$ and $\mathbf{C}$ are mass and damping matrices of $n \times n$, respectively, $\mathbf{f}$ is a linear or nonlinear force vector of $n \times 1$. The displacement, velocity, and acceleration of $n \times 1$ are denoted by $\boldsymbol{X}$, $\dot{\boldsymbol{X}}$, and $\ddot{\boldsymbol{X}}$, respectively. $\boldsymbol{\xi}$ is the loading influence matrix of $n \times 1$. In this paper, the uncertainty denoted by $\boldsymbol{\Theta}$ from the earthquake ground motions is taken into account, while the structure is considered to be deterministic.

Let $X(t)$ be the QoI that is a function of structural responses, i.e., $X(t) = g(\boldsymbol{X}, \dot{\boldsymbol{X}}, \ddot{\boldsymbol{X}})$ where $g(\cdot)$ is a linear or nonlinear mapping. For instance, The maximum inter-story drift or the top displacement may be of interest in seismic reliability assessment for building structures. In this paper, the QoI is defined as $X = \max_{t=0}^{T}\{|X_{\text{top}}(t)|\}$, where $X_{\text{top}}(t)$ is the time history of the structural top displacement. For most well-posed engineering systems, $X(t)$ is a unique function that exists as a function of $\boldsymbol{\Theta}$, which can be expressed by

$$X(t) = H(\boldsymbol{\Theta}, t), \;\; \dot{X}(t) = h(\boldsymbol{\Theta}, t) \tag{6}$$

where $h = \partial H/\partial t$ stands for the generalized velocity. Then, based on the principle of probability preservation[46], the joint PDF of $(X, \boldsymbol{\Theta})$ is governed by[2]

$$\frac{\partial p_{X\boldsymbol{\Theta}}(x, \boldsymbol{\theta}, t)}{\partial t} + h(\boldsymbol{\Theta}, t)\frac{\partial p_{X\boldsymbol{\Theta}}(x, \boldsymbol{\theta}, t)}{\partial x} = 0 \tag{7}$$

which is referred to as the generalized density evolution equation (GDEE). Finally, the PDF of QoI can be calculated by integrating $\boldsymbol{\theta}$ after solving Equation (7), i.e.,

$$p_X(x,t) = \int_{\Omega_{\boldsymbol{\Theta}}} p_{X\boldsymbol{\Theta}}(x,\boldsymbol{\theta},t)\mathrm{d}\boldsymbol{\theta} \tag{8}$$

where $\Omega_{\boldsymbol{\Theta}}$ is the sample space of $\boldsymbol{\Theta}$.

In general, the numerical algorithm of the PDEM consists of the following four steps:

Step 1.1. Generation of representative points. Denote $\Omega_{\boldsymbol{\Theta}}$ be partitioned into N disjoint subdomains satisfying $\cup_{q=1}^{N}\Omega_q = \Omega_{\boldsymbol{\Theta}}$ and $\Omega_p \cap \Omega_q = \emptyset$ for $p \neq q$ and $p,q = 1,2,\cdots,N$. For each subdomain Ω_q, select one representative point $\boldsymbol{\theta}_q \in \Omega_q$ and calculate its assigned probability P_q defined by

$$P_q = \int_{\Omega_q} p_{\boldsymbol{\Theta}}(\boldsymbol{\theta})\mathrm{d}\boldsymbol{\theta}. \tag{9}$$

The way to partition the sample space can be referred to Chen *et al.* (2009)[47]. Besides, to minimize the point discrepancy of representative points, the GF-discrepancy minimization strategy[48] is adopted in this work.

Step 1.2. For each $\boldsymbol{\Theta} = \boldsymbol{\theta}_q$, generate the stochastic ground motion $a_R(\boldsymbol{\theta}_q,t)$ by Equations (1) to (3). Then, solve Equation (5) and Equation (6) to obtain the generalized velocity $h(\boldsymbol{\theta}_q,t)$.

Step 1.3. For each $\boldsymbol{\Theta} = \boldsymbol{\theta}_q$, solve Equation (7) in a discretized version, i.e.,

$$\frac{\partial p_{X\boldsymbol{\Theta}}^{(q)}(x,\boldsymbol{\theta}_q,t)}{\partial t} + h(\boldsymbol{\theta}_q,t)\frac{\partial p_{X\boldsymbol{\Theta}}^{(q)}(x,\boldsymbol{\theta}_q,t)}{\partial x} = 0 \tag{10}$$

with the initial condition $p_{X\boldsymbol{\Theta}}^{(q)}(x,\boldsymbol{\theta}_q,t_0) = \delta_{\mathrm{D}}[x-x_0]P_q$ where $\delta_{\mathrm{D}}[\cdot]$ is the Dirac delta function. Equation (10) is a typical partial differential equation that can be numerically solved via finite difference methods[45].

Step 1.4. Assemble the results in **Step 1.3**, i.e., $p_X(x,t) = \sum_{q=1}^{N} p_{X\boldsymbol{\Theta}}^{(q)}(x,\boldsymbol{\theta}_q,t)$.

2.3 Uncertainty propagation via the change of probability measure

The aforementioned PDEM is available only if the input PDF is precisely determined. In other words, when the input PDF denoted by $p_{\boldsymbol{\Theta}}^{(1)}(\boldsymbol{\theta})$ is already known, the corresponding output PDF denoted by $p_X^{(1)}(x,t)$ can be accurately estimated by the PDEM. What if the PDF of $\boldsymbol{\Theta}$ is changed from $p_{\boldsymbol{\Theta}}^{(1)}(\boldsymbol{\theta})$ to $p_{\boldsymbol{\Theta}}^{(2)}(\boldsymbol{\theta})$? To obtain the PDF of X denoted by $p_X^{(2)}(x,t)$ in terms of $p_{\boldsymbol{\Theta}}^{(2)}(\boldsymbol{\theta})$, one may complement the probability density evolution analysis again, which undoubtedly requires another loop of deterministic analyses. To avoid additional model evaluations, the COM[4] is briefly introduced in this section. The combination of PDEM and COM is essential for a quick Fre-GSA in Section 2.4.

The backbone of the COM is based on the Radon-Nikodým theorem, which ensures that

$$p_X^{(2)}(x,t) = \mathcal{T} \circ p_X^{(1)}(x,t) \tag{11}$$

where $\circ$ means an operator on a function and $\mathcal{T}$ is the Radon-Nikodým derivative defined by

$$\mathcal{T} = \frac{\mathrm{d}P_{\boldsymbol{\Theta}}^{(2)}(\boldsymbol{\theta})}{\mathrm{d}P_{\boldsymbol{\Theta}}^{(1)}(\boldsymbol{\theta})} \tag{12}$$

where $P_{\boldsymbol{\Theta}}^{(2)}(\boldsymbol{\theta})$ and $P_{\boldsymbol{\Theta}}^{(1)}(\boldsymbol{\theta})$ are the cumulative distribution functions (CDFs) in terms of $p_{\boldsymbol{\Theta}}^{(2)}(\boldsymbol{\theta})$ and $p_{\boldsymbol{\Theta}}^{(1)}(\boldsymbol{\theta})$, respectively. Note that Equation (11) means one can obtain $p_X^{(2)}(x,t)$ directly by using the Radon-Nikodým derivative $\mathcal{T}$ rather than adding additional deterministic analyses.

For some simple stochastic systems, the analytical formula of Radon-Nikodým derivative can be found in Chen & Wan (2019)[4]. Nevertheless, it is always impossible to obtain an exact expression of Radon-Nikodým derivative for complex and nonlinear stochastic systems, but the COM can be numerically accomplished with the aid of the PDEM.

The numerical algorithm of the PDEM-COM is summarized as follows:

Step 2.1. Complete one round of probability density evolution analysis via PDEM introduced in Section 2.2. Store the point set $\mathcal{M}^{(1)} = \{\boldsymbol{\theta}_q^{(1)}, P_q^{(1)}\}_{q=1}^N$ and the corresponding generalized velocity $h(\boldsymbol{\theta}_q^{(1)}, t)$, where $\boldsymbol{\theta}_q^{(1)}$ is the q-th representative point with respect to the PDF $p_{\boldsymbol{\Theta}}^{(1)}(\boldsymbol{\theta})$.

Step 2.2. Considering the input PDF is changed from $p_{\boldsymbol{\Theta}}^{(1)}(\boldsymbol{\theta})$ to $p_{\boldsymbol{\Theta}}^{(2)}(\boldsymbol{\theta})$, recalculate the assigned probability by

$$P_q^{(2)} = \int_{\Omega_q^{(1)}} p_{\boldsymbol{\Theta}}^{(2)}(\boldsymbol{\theta})\mathrm{d}\boldsymbol{\theta},\ q = 1, 2, \cdots, N \tag{13}$$

where $\Omega_q^{(1)}$'s are the Voronoi cells determined by $\boldsymbol{\theta}_q$'s. This generates a new point set $\mathcal{M}^{(2)} = \{\boldsymbol{\theta}_q^{(1)}, P_q^{(2)}\}_{q=1}^N$. By doing so, the location of the q-th representative point is unchanged (still $\boldsymbol{\theta}_q^{(1)}$), which means the generalized velocity $h(\boldsymbol{\theta}_q^{(1)}, t)$ can be reused.

Step 2.3. Solve the GDEE in Equation (10) with a new initial condition $p_{X\boldsymbol{\Theta}}^{(q)}(x, \boldsymbol{\theta}_q^{(1)}, t_0) = \delta_{\mathrm{D}}[x - x_0]P_q^{(2)}$ and then assemble the results.

It should be emphasized that the accuracy of the PDEM-COM depends on whether the support of $p_{\boldsymbol{\Theta}}^{(1)}(\boldsymbol{\theta})$ mostly covers that of $p_{\boldsymbol{\Theta}}^{(2)}(\boldsymbol{\theta})$. When the supports of $p_{\boldsymbol{\Theta}}^{(1)}(\boldsymbol{\theta})$ and $p_{\boldsymbol{\Theta}}^{(2)}(\boldsymbol{\theta})$ are largely coincident, the PDEM-COM provides relatively accurate results. Nonetheless, if the supports of $p_{\boldsymbol{\Theta}}^{(1)}(\boldsymbol{\theta})$ and $p_{\boldsymbol{\Theta}}^{(2)}(\boldsymbol{\theta})$ are exclusive, for example, $\Omega_\Theta^{(1)} = (-1, 0)$ while $\Omega_\Theta^{(2)} = (0, 1)$, the accuracy of the PDEM-COM may immediately collapse because there is no universally perfect method. To address this issue, the accuracy of the PDEM-COM can be remarkably improved by an augmenting method. For more details, please refer to Wan *et al.* (2023)[49].

2.4 Fréchet-derivative-based global sensitivity analysis

The Fre-GSA provides a quantitative approach to identify the most influential variables of input for stochastic systems. In this analysis, a Fre-GSI is calculated, and its parametric form is defined by[43]

$$\mathcal{F}_\psi(x, t; \boldsymbol{\xi}) = \frac{\partial p_X(x, t; \boldsymbol{\xi})/\partial \boldsymbol{\xi}}{\|\partial p_{\boldsymbol{\Theta}}(\boldsymbol{\theta}; \boldsymbol{\xi})/\partial \boldsymbol{\xi}\|} \tag{14}$$

and the j-th Fre-GSI reads

$$\mathcal{F}_{\psi,j}(x, t; \boldsymbol{\xi}) = \frac{\partial p_X(x, t; \boldsymbol{\xi})/\partial \xi_j}{\left\|\partial p_{\Theta_i}(\theta_i; \boldsymbol{\xi})/\partial \xi_j\right\|},\ j = 1, 2, \cdots, m \tag{15}$$

where ξ_j is the j-th distribution parameter of the i-th random variable Θ_i, and the norm term in the denominator is defined as $\|p\| = \frac{1}{2}\int |p|$. It should be emphasized that Equation (15) holds on the assumption that ξ_j's are independent. Specifically, in the studied StoModel, Θ_i is associated with $\boldsymbol{\xi} = \{a_i, b_i\}$ where $i = 1, 2, 3, 4$ for Site I, Site II, Site III, and Site IV.

For the j-th Fre-GSI, the corresponding IM is given by[50]

$$\mathcal{S}_j = \left\|\mathcal{F}_{\psi,j}\right\|,\ j = 1, 2, \cdots, m, \tag{16}$$

which theoretically satisfies that $0 \leq \mathcal{S}_j \leq 1$.

The j-th Fre-GSI can be calculated via the PDEM-COM in Section 2.3, which mainly consists of three steps:

Step 3.1. Firstly, calculate $p_X(x, t; \boldsymbol{\xi})$ with respect to $p_{\boldsymbol{\Theta}}(\boldsymbol{\theta}; \boldsymbol{\xi})$ via the PDEM, in which the point set $\mathcal{M} = \{\boldsymbol{\theta}_q, P_q\}_{q=1}^N$ and the corresponding generalized velocity $h(\boldsymbol{\theta}_q, t)$ are stored.

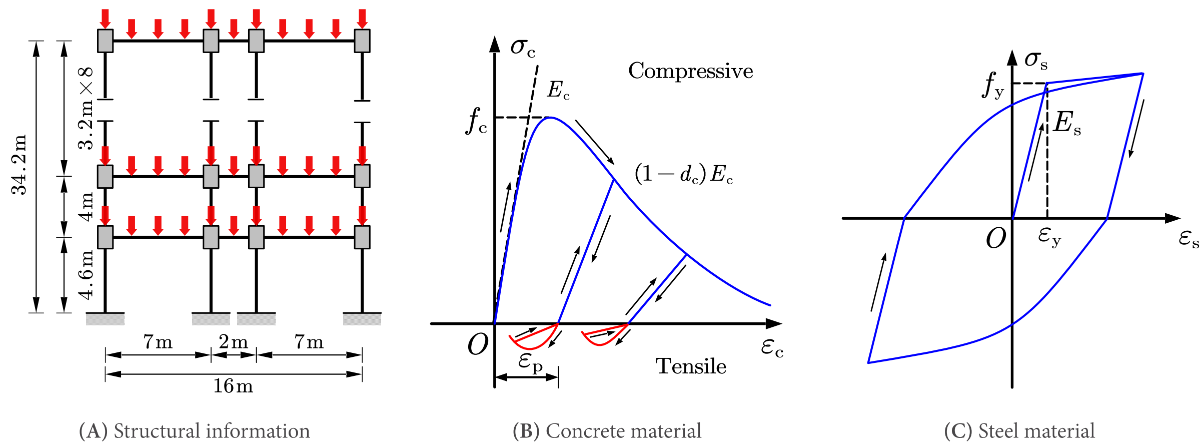

Figure 2. A 10-story reinforced concrete frame structure [4,5].

Step 3.2. Calculate $p_X(x, t; \boldsymbol{\xi} + \boldsymbol{e}_j \Delta\xi_j)$ and $p_X(x, t; \boldsymbol{\xi} - \boldsymbol{e}_j \xi_j)$ in terms of $p_{\boldsymbol{\Theta}}(\boldsymbol{\theta}; \boldsymbol{\xi} + \boldsymbol{e}_j \Delta\xi_j)$ and $p_{\boldsymbol{\Theta}}(\boldsymbol{\theta}; \boldsymbol{\xi} - \boldsymbol{e}_j \Delta\xi_j)$, respectively, where $\boldsymbol{e}_j$ is a selection vector whose elements are zeros except its j-th location equal to one, and $\Delta\xi$ is a small perturbation, e.g., $\Delta\xi = 0.01$ for $\xi_j = 0$ and $\Delta\xi_j = 0.01\xi_j$ for $\xi_j \neq 0$. Note that this step can be speedily accomplished by adopting the PDEM-COM, as mentioned in Section 2.3.

Step 3.3. Approximate the j-th Fre-GSI via a central difference scheme, i.e.,

$$\mathcal{F}_{\psi,j}(x, t; \boldsymbol{\xi}) \approx \frac{1}{2} \frac{p_X(x, t; \boldsymbol{\xi} + \boldsymbol{e}_j \Delta\xi_j) - p_X(x, t; \boldsymbol{\xi} - \boldsymbol{e}_j \Delta\xi_j)}{\Delta\xi_j} / \left\| \partial p_{\Theta_i}(\theta_i; \boldsymbol{\xi}) / \partial \xi_j \right\| \tag{17}$$

where the norm term in the denominator can be numerically or analytically computed [4].

3. ENGINEERING APPLICATION

The aim of this paper is to investigate how the distribution parameters of the StoModel may affect the stochastic responses of the structure by adopting the Fre-GSA. To achieve this goal, a 10-story reinforced concrete frame structure, as shown in Figure 2A, is considered. The finite element model of the structure is modeled via the OpenSees software. The constitutive model of concrete materials is described by the elastoplastic damage constitutive model [51] (ConcreteD command), which is consistent with the Chinese design code (GB 50010-2010) [52]. The behavior of steel materials is characterized via the Giuffré-Menegotto-Pinto model [53] (Steel02 command), which accounts for the effect of isotropic strengthening. The stress-strain curves of the concrete and steel materials are shown in Figure 2B and Figure 2C, respectively. The labels "Compressive" and "Tensile" stand for the compressive state and the tensile state of the concrete materials, respectively.

Assume the seismic fortification intensity is categorized as 8.0, and the design basic acceleration of ground motion with a 10% exceedance probability of 50 years is $0.30g$, where g is the acceleration of gravity. According to the Chinese design code (GB 50011-2010) [44], the peak ground accelerations (PGAs) of the transient dynamic analysis are assigned to 110 cm/sec^2 and 510 cm/sec^2 for the frequent earthquake and rare earthquake, respectively.

Comparisons of the dynamic amplification coefficients via the StoModel and the Chinese design code [44] for four site classes are drawn in Figure 3. Note that in Figure 3, the Y-axis β stands for the dynamic amplification coefficient, which means the amplitudes of all generated ground motions are normalized to one before the analysis. A total of 300 representative points are generated for each site classification (Table 1) via the GF-discrepancy minimization strategy [48]. The results show that the mean response obtained from the StoModel

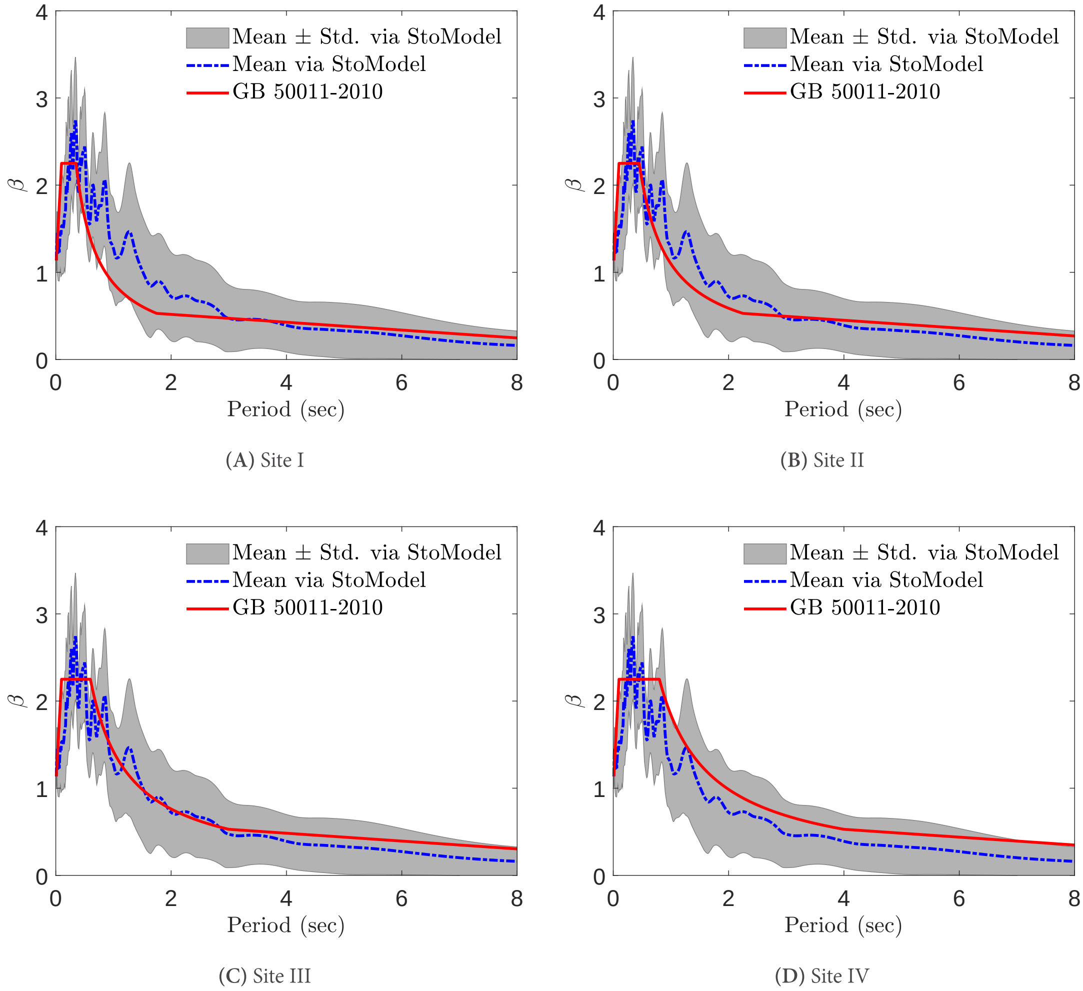

Figure 3. Comparisons of the dynamic amplification coefficients via the physical random function model of ground motions (StoModel) and the Chinese design code (GB 50011-2010) [44].

is basically consistent with the one from the design code, and the range of the StoModel (mean value ± standard deviation) can effectively cover the curve (red solid line) via the design code. It should be noted that in the Chinese design code, the value of the dynamic amplification coefficient in the long-period interval is artificially lifted to account for the long-period effect on structural responses. However, by adopting a stochastic ground-motion model, this effect can be naturally taken into account.

The results for the case of a frequent earthquake (PGA= 110 cm/sec^2) are shown in Figure 4 and Figure 5, where the Fre-GSIs of distribution parameters of the StoModel are presented in Figure 4, and the corresponding IMs are drawn in Figure 5. Observing Figure 5, it can be seen that the shape of the distribution for the PDF of the extreme top displacement becomes flatter as we move from Site I to Site IV. Additionally, the Fre-GSIs become more complex. More specifically, it is seen that a small increase of parameter a_4 or b_4 will make the PDF of the extreme top displacement move to the left. This behavior is intuitively reasonable because a larger a_4 or b_4 will make the PDF of ω_g (the equivalent predominate circular frequency of the site) become flatter (see Figure 1D), which means that the probability of obtaining a lower realization of ω_g close to the natural frequency of the structure has decreased. In this study, the natural frequency of the 10-story reinforced concrete frame structure is 6.78 Hz. Moreover, the IMs in Figure 5 indicate that ω_g provides the greatest contribution to the PDF of

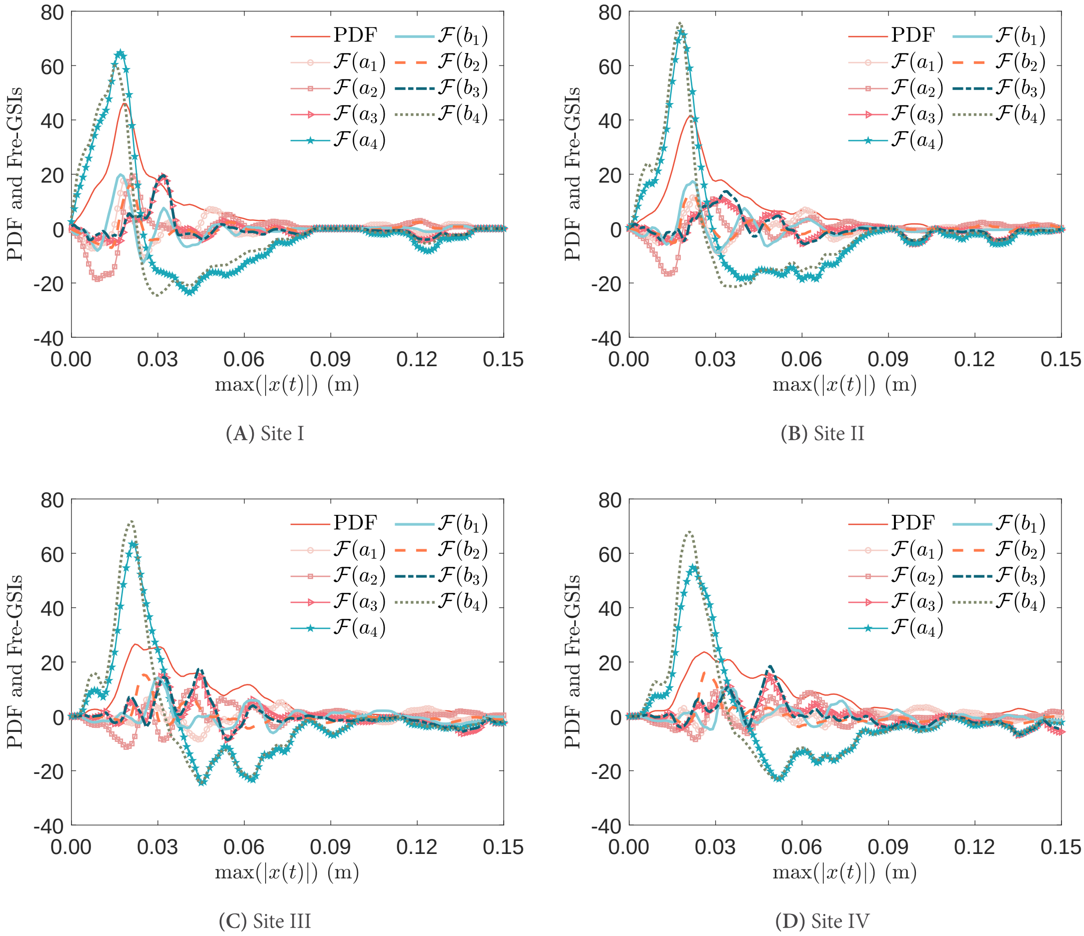

Figure 4. The Fre-GSIs of the StoModel considering four sites (frequent earthquake).

the extreme top displacement (IM is greater than 0.8), which significantly surpasses the contributions of other parameters, such as A_0, τ, and ζ_g, whose IMs are all around 0.2.

In contrast to the case of a frequent earthquake, the PDF of the extreme top displacement becomes sharper as we move from Site I to Site IV, while the amplitudes of the Fre-GSIs turn out to be smaller. This difference may be attributed to the much stronger development of the structural nonlinearity in the case of a rare earthquake, as shown in Figure 6.The results for the rare earthquake (PGA= 510 cm/sec^2) are shown in Figure 7 for the Fre-GSIs and in Figure 8 for the IMs. Similar to the case of a frequent earthquake, the Fre-GSIs with respect to the parameters a_4 and b_4 have the greatest impact on the PDF of the extreme top displacement. However, for the rare earthquake case, the Fre-GSI related to the parameter a_2 also has a significant effect. According to Figure 7, the Fre-GSI in terms of a_2 indicates that a fairly small incremental change of a_2 would result in a rightward shift in the PDF of the extreme top displacement. The physical interpretations for this result are: It is noted that a_2 is the distribution parameter of τ, which is the Brune source parameter that characterizes the decay process of the fault rupture. Therefore, a larger a_2 corresponds to a flatter distribution of τ (see Figure 1B), which means a higher possibility of having a larger realization of τ. Comparing the results in Figure 7 and Figure 8 with those in Figure 4 and Figure 5, it is found that even for the same deterministic structure, the sensitivity of structural responses to the parameters of the StoModel can vary significantly due to the coupling effect of randomness and nonlinearity[2].

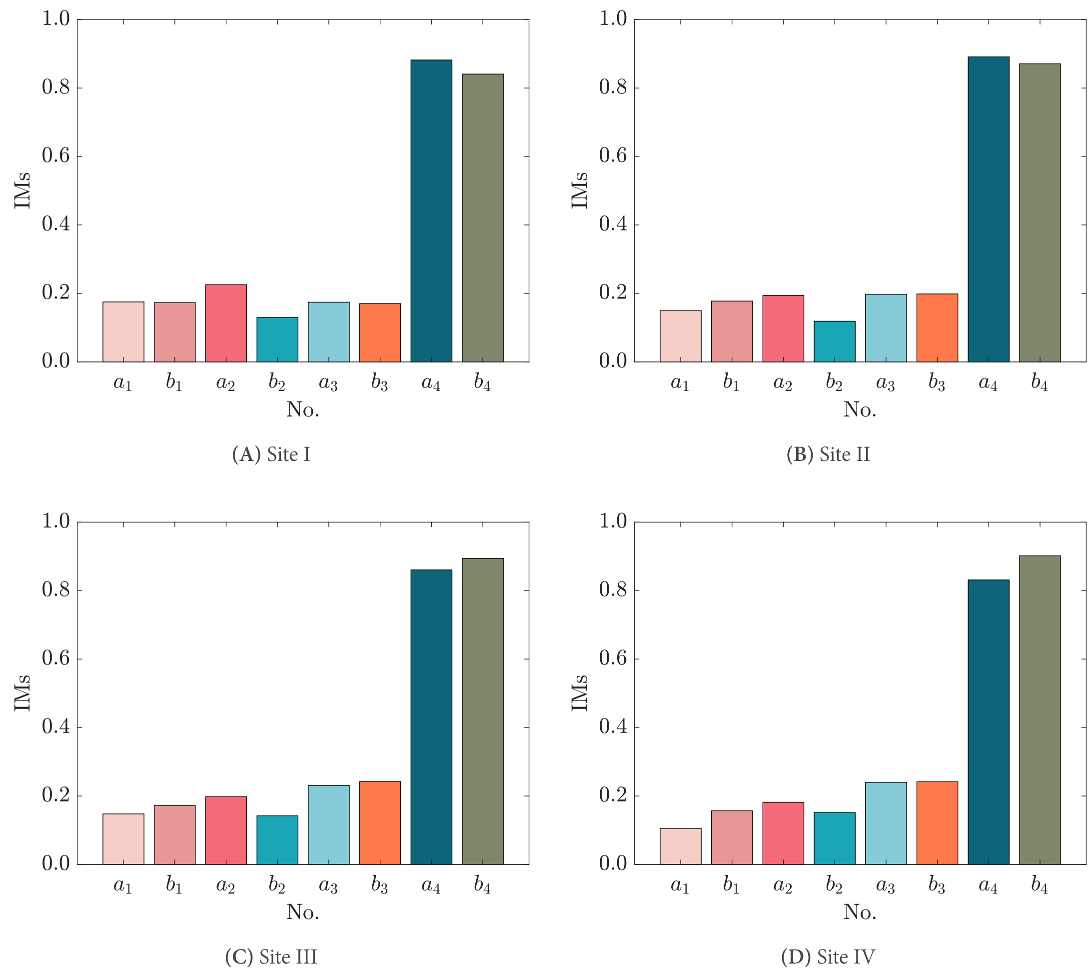

Figure 5. The IMs of the StoModel considering four sites (frequent earthquake).

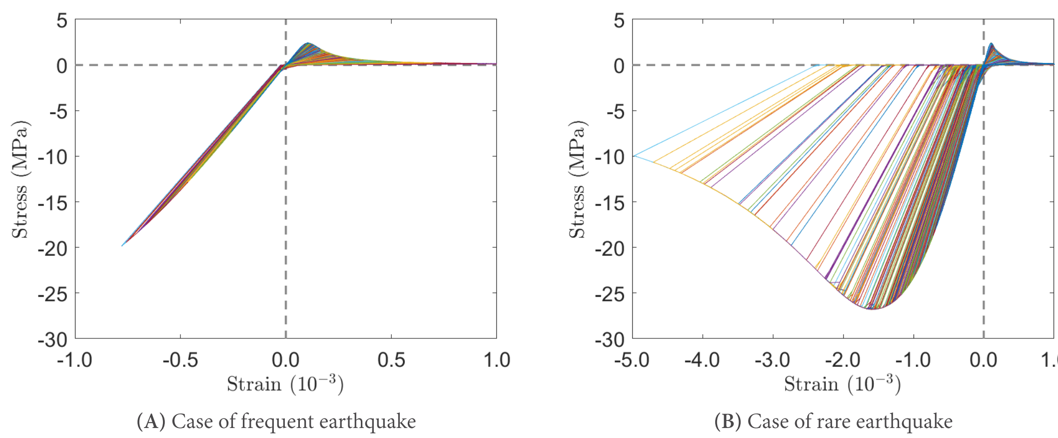

Figure 6. Typical stress-strain curves of concrete materials.

4. CONCLUSIONS

In this paper, We investigate the sensitivity of parameters in the StoModel by measuring the Fre-GSI. Numerical computation of the Fre-GSI is sharply accelerated by integrating the PDEM and the COM. As a benchmark

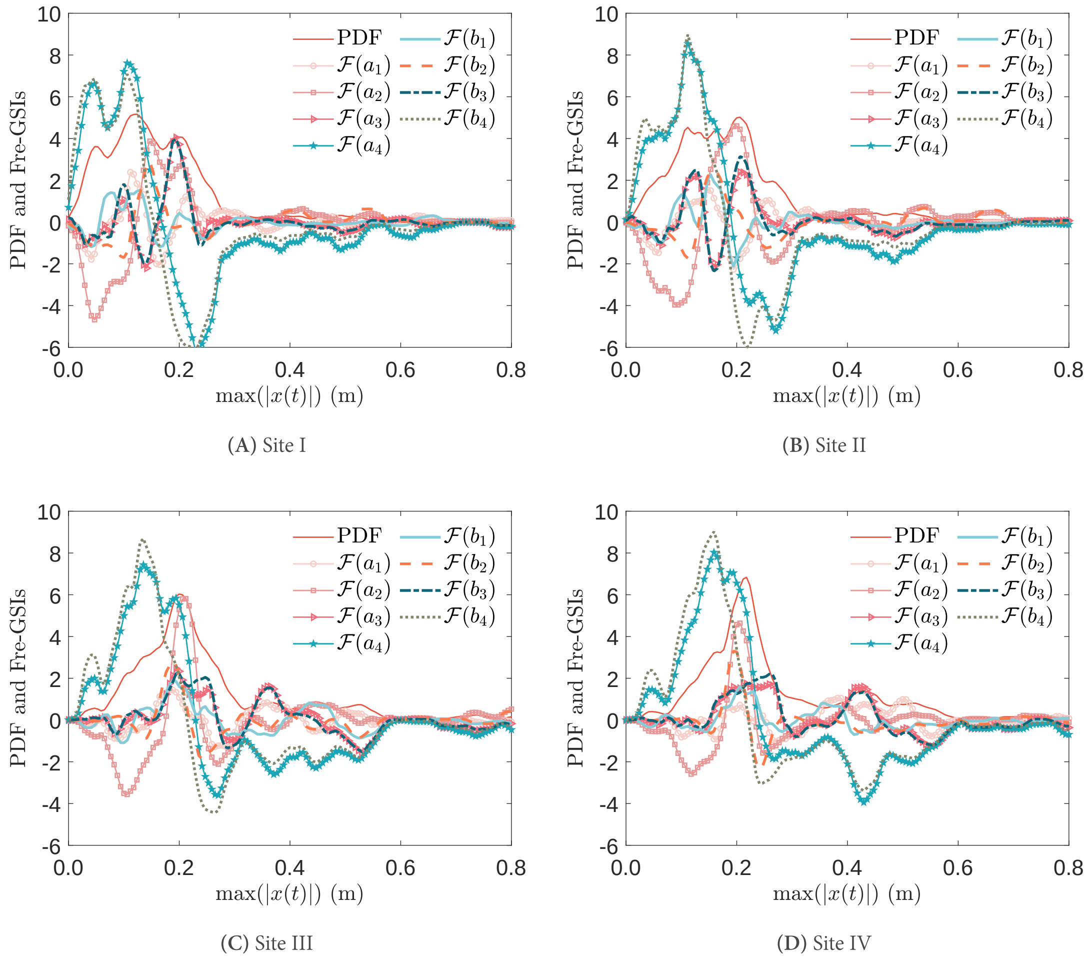

Figure 7. The Fre-GSIs of the StoModel considering four sites (rare earthquake).

model, we analyze a 10-story reinforced concrete frame structure while considering the consistency of the StoModel with the Chinese design code (GB 50011-2010)[44]. The main conclusions of this study are as follows:

1. The StoModel is statistically consistent with the Chinese design code, in terms of the dynamic amplification coefficient.
2. Once the PDF of the QoI is estimated by the PDEM, the Fre-GSI can be obtained as a byproduct that can be rapidly computed via the COM.
3. For the case of a frequent earthquake, when the mechanical behavior of the structure is nearly linear, the parameter ω_g (equivalent predominate circular frequency) in the StoModel is the dominant parameter, whose IM (= 0.8) is significantly higher than those of the other three model parameters.
4. For the case of a rare earthquake, when the structure enters a highly nonlinear stage, although ω_g remains the most influential parameter, the IM of the Brune source parameter τ nearly doubles, increasing from around 0.2 to around 0.4. This indicates that the change in the physical state of the structure may trigger the change of IMs of the basic inputs.
5. It is suggested that more information on the parameters ω_g and τ (especially ω_g) should be obtained to enhance the robustness of the StoModel.

More research is needed to address certain issues. For instance, studies are still being conducted to better describe the randomness of ground motions using more realistic physical random functions and to take into

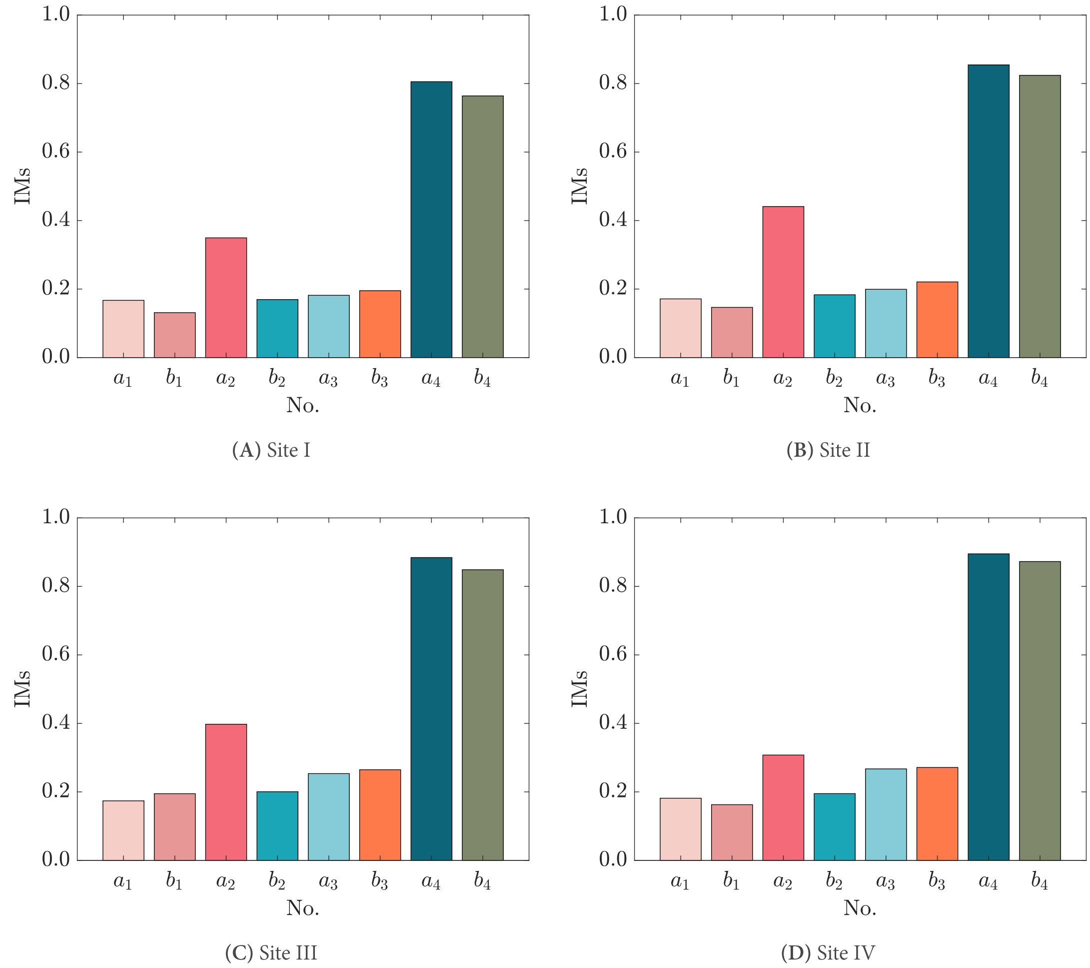

Figure 8. The IMs of the StoModel considering four sites (rare earthquake).

account the inherent uncertainty in structural parameters. Additionally, the adopted ground-motion model in this paper also needs further improvements, particularly in aspects related to the physical mechanisms of the source model, path model, local-site effects, etc. Moreover, model uncertainty of the ground-motion model is a concerning factor that requires attention in future research efforts.

DECLARATIONS

Acknowledgments

The financial support provided by the National Natural Science Foundation of China (NSFC Grant No. 52208206) and the Fundamental Research Funds for the Central Universities (Grant Nos. G2022KY05103) is highly appreciated.

Authors' contributions

Conceptualization, Investigation, Methodology, Formal analysis, Software, Writing - original draft, and Writing - review & editing: Wan Z

Resources, Funding acquisition, and Data curation: Tao W, Ding Y, Xin L

Availability of data and materials

Some or all of the data, models, or code generated or used during the study are available from the author upon request.

Financial support and sponsorship

The National Natural Science Foundation of China (NSFC Grant No. 52208206);
The Fundamental Research Funds for the Central Universities (Grant Nos. G2022KY05103).

Conflicts of interest

All authors declared that there are no conflicts of interest.

Ethical approval and consent to participate

Not applicable.

Consent for publication

Not applicable.

REFERENCES

1. Ang AHS, Tang W. Probability concepts in engineering: emphasis on applications to civil and environmental engineering. John Wiley & Sons; 2007.
2. Chen JB, Li J. Stochastic seismic response analysis of structures exhibiting high nonlinearity. *Comput Struct* 2010;88:395–412. DOI
3. Zhou H, Li J, Ren XD. Multi-scale stochastic structural analysis toward reliability assessment for large complex reinforced concrete structures. *Int J Multiscale Comput* 2016;14:303–21. DOI
4. Chen JB, Wan ZQ. A compatible probabilistic framework for quantification of simultaneous aleatory and epistemic uncertainty of basic parameters of structures by synthesizing the change of measure and change of random variables. *Struct Saf* 2019;78:76–87. DOI
5. Wan ZQ, Chen JB, Li J. Probability density evolution analysis of stochastic seismic response of structures with dependent random parameters. *Probabilistic Eng Mech* 2020;59:103032. DOI
6. Chen KH, Pang R, Xu B. Stochastic dynamic response and seismic fragility analysis for high concrete face rockfill dams considering earthquake and parameter uncertainties. *Soil Dyn Earthq Eng* 2023;167:107817. DOI
7. Cao XY, Feng DC, Beer M. Consistent seismic hazard and fragility analysis considering combined capacity-demand uncertainties via probability density evolution method. *Struct Saf* 2023;103:102330. DOI
8. Yu XH, Li S, Lu DG, Tao J. Collapse capacity of inelastic single-degree-of-freedom systems subjected to mainshock-aftershock earthquake sequences. *J Earthq Eng* 2020;24:803–26. DOI
9. Feng DC, Cao XY, Wang D, Wu G. A PDEM-based non-parametric seismic fragility assessment method for RC structures under non-stationary ground motions. *J Build Eng* 2023;63:Part A. DOI
10. Chen Y, Patelli E, Edwards B, Beer M. A physics-informed Bayesian framework for characterizing ground motion process in the presence of missing data. *Earthq Eng Struct Dyn* 2023; 52:2179–95. DOI
11. Brune JN. Tectonic stress and the spectra of seismic shear waves from earthquakes. *J Geophys Res* 1970;75:4997–5009. DOI
12. Das S, Aki K. Fault plane with barriers: A versatile earthquake model. *J Geophys Res* 1977;82:5658–70. DOI
13. Wang GX, Li YN. Strong ground motion simulation for recent earthquakes in China. Proceedings of the 16th World Conference on Earthquake Engineering; 2017 Jan 9-13; Santiago, Chile. Available from: http://wcee.nicee.org/wcee/article/16WCEE/WCEE2017-3036.pdf. [Last accessed on 22 April 2023]
14. Okuwaki R, Yagi Y. Role of geometric barriers in irregular-rupture evolution during the 2008 Wenchuan earthquake. *Geophys J Int* 2018;212:1657–64. DOI
15. Housner GW. Characteristics of strong-motion earthquakes. *Bull Seismol Soc Am* 1947;37:19–31. DOI
16. Kanai K. Semi-empirical formula for the seismic characteristics of the ground. *Bull Earthq Res Inst Univ Tokyo* 1957;35:309–25. DOI
17. Tajimi H. A statistical method of determining the maximum response of a building structure during an earthquake. Proceedings of the 2nd World Conference on Earthquake Engineering; 1960 July 11-18; Tokyo, Japan. Available from: https://www.iitk.ac.in/nicee/wcee/article/vol.2_session2_781.pdf. [Last accessed on 22 April 2023]
18. Hu YX, Zhou XY. The Response of the Elastic System under the Stationary and Nonstationary Ground Motions. Beijing: Science Press; 1962.
19. Ou JP, Niu DT. Parameters in the random process models of earthquake ground motion and their effects on the response of structures. *J*

Harbin Archit Civ Eng Inst 1990;23:24–34. Available from: https://kns.cnki.net/KCMS/detail/detail.aspx?dbcode=CJFD&filename=HEBJ199002002. [Last accessed on 22 April 2023]
20. Clough RW, Penzien J. Dynamics of Structures. 3rd ed. Berkeley: Computers & Structures, Inc.; 1995.
21. Amin M, Ang AHS. Nonstationary stochastic models of earthquake motions. *J Eng Mech Div* 1968;94:559–84. DOI
22. Li C, Li HN, Hao H, Bi K, Tian L. Simulation of multi-support depth-varying earthquake ground motions within heterogeneous onshore and offshore sites. *Earthq Eng Eng Vib* 2018;17:475–90. DOI
23. Wang D, Li J. Physical random function model of ground motions for engineering purposes. *Sci China Technol Sci* 2011;54:175–82. DOI
24. Wang D, Li J. A random physical model of seismic ground motion field on local engineering site. *Sci China Technol Sci* 2012;55:2057–65. DOI
25. Ding YQ, Peng YB, Li J. A stochastic semi-physical model of seismic ground motions in time domain. *J Earthq Tsunami* 2018;12:1850006. DOI
26. Ding YQ, Xu YZ, Miao HQ. A seismic checking method of engineering structures based on the stochastic semi-physical model of seismic ground motions. *Buildings* 2022;12:488. DOI
27. Li C, Hao H, Li HN, Bi KM. Theoretical modeling and numerical simulation of seismic motions at seafloor. *Soil Dyn Earthq Eng* 2015;77:220–25. DOI
28. Li C, Hao H, Li HN, Bi KM, Chen BK. Modeling and simulation of spatially correlated ground motions at multiple onshore and offshore sites. *J Earthq Eng* 2017;21:359–83. DOI
29. Li C, Li HN, Hao H, Bi KM, Chen BK. Seismic fragility analyses of sea-crossing cable-stayed bridges subjected to multi-support ground motions on offshore sites. *Eng Struct* 2018;165:441–56. DOI
30. Li C, Li HN, Hao H, Bi KM. Simulation of spatially varying seafloor motions using onshore earthquake recordings. *J Eng Mech* 2018;144:04018085. DOI
31. Li J, Ai XQ. Study on random model of earthquake ground motion based on physical process. *Earthq Eng Eng Vib* 2006;26:21–26. DOI
32. Li J, Wang D. Parametric statistic and certification of physical stochastic model of seismic ground motion for engineering purposes. *Earthq Eng Eng Vib* 2013;33:81–88. DOI
33. Li ZC, Liu W. Parametric statistics and validation of Wenchuan earthquake based on physical stochastic model of ground motion. *Struct Eng* 2015;31:69–74. DOI
34. Saltelli A, Tarantola S, Campolongo F, Ratto M. Sensitivity Analysis in Practice: A Guide to Assessing Scientific Models. New York: John Wiley & Sons; 2004. DOI
35. Sobol' IM. Sensitivity estimates for nonlinear mathematical models. *Math Model Comput Expe* 1993;1:407–14.
36. Wei PF, Lu ZZ, Song JW. A new variance-based global sensitivity analysis technique. *Comput Phys Commun* 2013;184:2540–51. DOI
37. Borgonovo E. A new uncertainty importance measure. *Reliab Eng Syst Saf* 2007;92:771–84. DOI
38. Wei PF, Lu ZZ, Yuan XK. Monte Carlo simulation for moment-independent sensitivity analysis. *Reliab Eng Syst Saf* 2013;110:6–67. DOI
39. Dubourg V, Sudret B. Meta-model-based importance sampling for reliability sensitivity analysis. *Struct Saf* 2014;49:27–36. DOI
40. Song JW, Wei PF, Valdebenito MA, Faes M, Beer M. Data-driven and active learning of variance-based sensitivity indices with Bayesian probabilistic integration. *Mech Syst Signal Process* 2022;163:108106. DOI
41. Phoon KK, Ching JY. Risk and Reliability in Geotechnical Engineering. Boca Raton: Taylor & Francis Group; 2015. DOI
42. Chen JB, Yang JS, Jensen H. Structural optimization considering dynamic reliability constraints via probability density evolution method and change of probability measure. *Struct Multidiscipl Optim* 2020;62:2499–516. DOI
43. Chen JB, Wan ZQ, Beer M. A global sensitivity index based on Fréchet derivative and its efficient numerical analysis. *Probabilistic Eng Mech* 2020;62:103096. DOI
44. Ministry of Housing and Urban-Rural Development of the People's Republic of China. Code for Seismic Design of Buildings GB 50011-2010. Beijing: China Architecture & Building Press; 2016.
45. Li J, Chen JB. Stochastic Dynamics of Structures. Singapore: John Wiley & Sons; 2009. DOI
46. Li J, Chen JB. The principle of preservation of probability and the generalized density evolution equation. *Struct Saf* 2008;30:65–77. DOI
47. Chen JB, Ghanem R, Li J. Partition of the probability-assigned space in probability density evolution analysis of nonlinear stochastic structures. *Probabilistic Eng Mech* 2009;24:27–42. DOI
48. Chen JB, Yang JY, Li J. A GF-discrepancy for point selection in stochastic seismic response analysis of structures with uncertain parameters. *Struct Saf* 2016;59:20–31. DOI
49. Wan ZQ, Hong X, Tao WF. Improvements to the probability density evolution method integrated with the change of probability measure on quantifying hybrid uncertainties. *Struct Saf* 2023;103:102342. DOI
50. Wan ZQ, Chen JB, Beer M. Functional perspective of uncertainty quantification for stochastic parametric systems and global sensitivity analysis. *Chin J Theor Appl Mech* 2021;53:837–54. DOI
51. Wan ZY, Ren XD, Li J. The implementation of uniaxial concrete constitutive model based on OpenSees. *Struct Eng* 2015;31:93–99. DOI
52. Ministry of Housing and Urban-Rural Development of the People's Republic of China. Code for Design of Concrete Structures GB 50010-2010. Beijing: China Architecture & Building Press; 2010.
53. Filippou FC, Popov EP, Bertero VV. Effects of Bond Deterioration on Hysteretic Behavior of Reinforced Concrete Joints. Berkeley: University of California; 1983. Available from: https://nehrpsearch.nist.gov/static/files/NSF/PB84192020.pdf. [Last accessed on 22 April 2023]